Korea-Australia Rheology Journal, 31(3), 141-147 (August 2019) www.springer.com/13367
DOI: 10.1007/s13367-019-0015-4

Three-dimensional numerical simulation for resin transfer molding of automotive wheel

Zheng Min Huang[1], So Yun Lee[1], Hyung Min Kim[1], Jae Ryoun Youn[1,*] and Young Seok Song[2,*]
[1]*Research Institute of Advanced Materials (RIAM), Department of Materials Science and Engineering, Seoul National University, Seoul 08826, Republic of Korea*
[2]*Department of Fiber System Engineering, Dankook University, Yongin 16890, Republic of Korea*

(Received May 1, 2019; final revision received June 18, 2019; accepted June 18, 2019)

Resin transfer molding (RTM) is a manufacturing process that uses liquid resin to saturate a fiber preform placed in a closed mold cavity. For robust fabrication of the composite, fiber preform needs to be completely impregnated with polymer resin during mold filling. Hence, the understanding of resin flow and void formation in RTM is very important to design the mold and processing conditions for successful production of composite parts. In this study, three-dimensional (3D) numerical simulation was carried out to investigate the resin flow behavior in a complicated mold. An automotive wheel rim was designed and fabricated using carbon fiber preform and epoxy resin. Case studies were performed to minimize the void formation during processing.

Keywords: resin transfer molding, void formation, numerical simulation

1. Introduction

In recent years, many studies have focused on improving fuel efficiency by using lightweight components in automotive industry. Indeed, weight reduction becomes an important issue due to high oil prices and strict fuel efficiency regulations. This can be achieved through several approaches: New structural design, processing, and materials. In particular, replacing existing heavy materials with lightweight materials can induce a big impact. However, the application of such composite materials to automotive parts is still limited due to their long processing cycle time and production cost (Chen *et al*., 2019).

Carbon fiber reinforced plastics (CFRPs) used in automobile are mostly manufactured using the resin transfer molding (RTM) process, which can fabricate complex structure and thick product (Bruschke and Advani, 1990; Laurenzi *et al.*, 2014; Yim *et al.*, 2018; Young *et al.*, 1991a; Young, 1994b). However, since various problems occur during manufacturing large and complex parts, numerical simulation of RTM can help design and optimize the process. In general, the simulation focuses on the filling step providing a guide regarding the processing conditions such as flow rate and pressure (Young *et al.*, 1991b). For example, by predicting the resin flow behavior, it can be determined whether or not a fiber preform is completely filled. In addition, the resin inlet and vent positions can be optimized based on the simulation result (Kim *et al.*, 2000; Young, 1994a). Since a number of products manufactured via RTM are simple and thin, it has been assumed that the flow in the thickness direction is neglected in the simulation (Chan and Hwang, 1988; 1991; 1992; Coulter and Guceri, 1988; Hattabi *et al.*, 2008; Li and Gauvin, 1991; Lin *et al.*, 1993; Yoo and Lee, 1996). However, it is necessary to carry out three-dimensional (3D) flow analysis to comprehend underlying physics regarding flow behavior in complex and thick parts produced using RTM (Bruschke and Advani, 1994; García-Manrique *et al.*, 2016; Isoldi *et al.*, 2012; Lee *et al.*, 1994; Oliveira *et al.*, 2015; Poodts *et al.*, 2014; Shojaei *et al.*, 2003; Trochu *et al.*, 1993).

In this study, numerical and experimental studies have been carried out to manufacture a large and complex CFRP part. As a representative part to substitute metallic parts, an automotive wheel rim was selected and fabricated (Fig. 1). The wheel rim is a component that can play an important role in reducing the weight of automobiles. 3D numerical simulation was conducted to investigate the resin flow behavior in the complex mold.

2. Modeling and Processing of RTM

2.1. Governing equations

Numerical analysis of RTM was carried out using finite element method. The filling process was simulated at constant temperature assuming that the resin was an incompressible and Newtonian fluid. Fiber preform generally has anisotropic permeability values depending on the fiber orientation. For a thin CFRP, the flow in the thickness direction is negligible compared with those in the other directions. Therefore, the permeability is considered as a 2D tensor. However, the out-of-plane permeability needs to be considered to manufacture thick composite parts

*Corresponding authors; E-mail: J.R. Youn (jaeryoun@snu.ac.kr) and Y.S. Song (ysong@dankook.ac.kr)

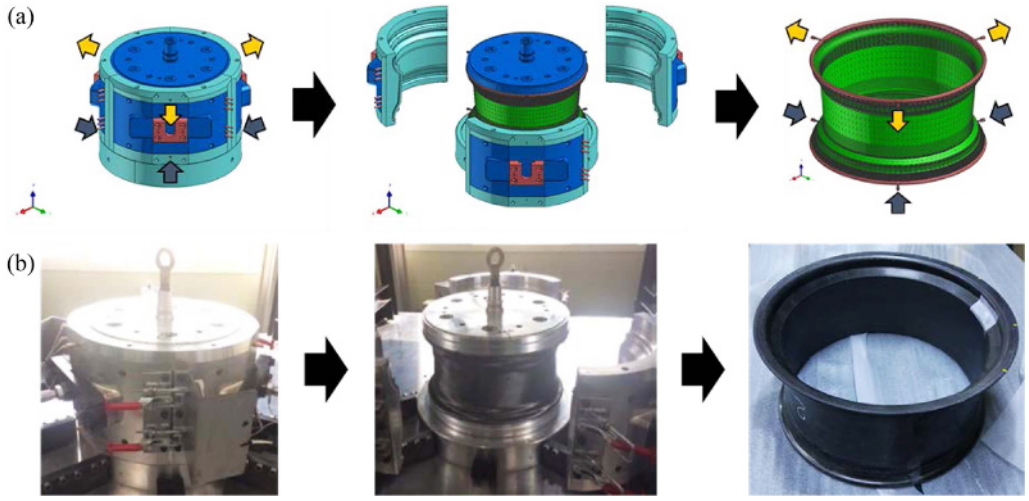

Fig. 1. (Color online) (a) Schematic illustration and (b) photographs of the mold and the CFRP.

since the flow in the thickness direction is meaningful. As a result, 3D modeling can provide more improved accuracy and reliability of results than 2D modeling. When the resin is incompressible fluid, pressure, and velocity fields are obtained by solving the following equations: Darcy's law (Eq. (1)) and continuity equation (Eq. (2)).

$$\mathbf{u} = \frac{\mathbf{K}}{\mu} \cdot \nabla \mathrm{P}\,, \tag{1}$$

$$\nabla \cdot \mathbf{u} = 0 \tag{2}$$

where $\mathbf{u}$ is the velocity vector of fluid, $\mathbf{K}$ is the permeability tensor of porous medium, μ is the Newtonian viscosity of fluid, and $\nabla \mathrm{P}$ is the pressure gradient vector.

Darcy's law can be integrated into continuity equation for incompressible fluid to obtain the pressure field as follows:

$$\nabla \cdot \left(\frac{\mathbf{K}}{\mu} \cdot \nabla \mathrm{P} \right) = 0\,. \tag{3}$$

A fill factor f is introduced to track the evolution of the flow front:

$$\frac{\partial f}{\partial t} + \nabla \cdot (\mathbf{u} f) = 0 \tag{4}$$

where $0 \le f < 1$ is defined as unsaturated region, so the pressure is $\mathrm{P} = 0$. $f = 1$ is defined as saturated region and the pressure is $\mathrm{P} \ge 0$.

The macro/micro-void formation is related to the flow velocity and flow front of resin. At low flow velocity, macro-voids tend to be generated, whereas high flow velocity leads to micro-void formation. The percentage of the macro- (Eq. (5)) and micro-voids (Eq. (6)) formation can be modeled as follows (Patel *et al.*, 1995; Ruiz *et al.*, 2006):

$$\mathbf{V}_{\mathrm{M}} = -1574 \cdot \mathbf{v} + 12.82\,, \tag{5}$$

$$\mathbf{V}_{\mathrm{m}} = -100.5 \cdot \mathbf{v} + 1.27 \tag{6}$$

where $\mathbf{v}$ is the component of the velocity vector.

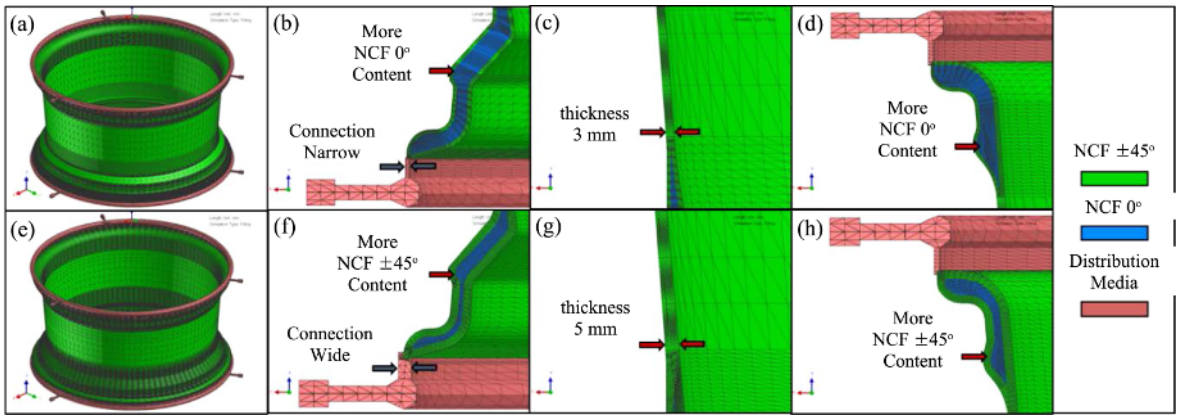

Fig. 2. (Color online) Overall geometry and magnified cross-section of the CFRP rim: (a) to (d) for Case 1 and (e) to (h) for Case 4.

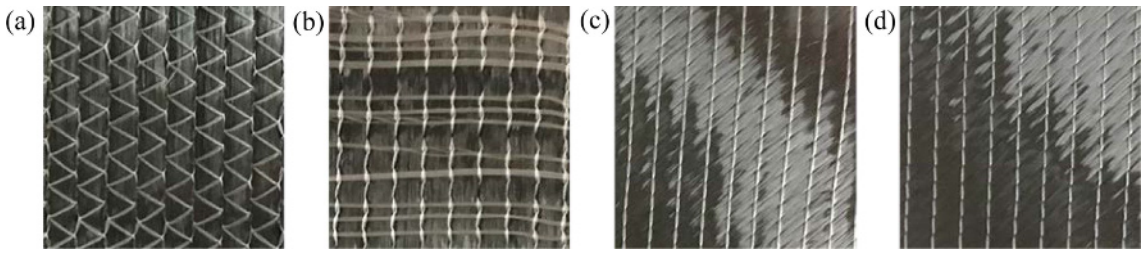

Fig. 3. (Color online) Photographs of the NCF used in this study. (a) Front side and (b) back side for the NCF 0º. (c) Front side and (d) back side for the NCF ± 45º.

In order to obtain more accurate void contents, it is preferable to conduct an experiment with same resin viscosity in advance to determine the equation. However, in this study, it is focused on whether improvements have been made between several cases rather than predicting the exact void contents value.

2.2. Geometric modeling

The geometrical structure of the CFRP wheel rim is shown in Fig. 2. The 3D model consisted of the preform parts (*i.e.*, the green and blue regions) and the distribution media part (*i.e.*, the brown region). The preform parts were occupied by two different non-crimp fabrics, NCF 0º and NCF ± 45º (Fig. 3). The NCF 0º had a low permeability and was placed inside the rim. The NCF ± 45º with a high permeability was located outside the rim. On the other hand, since the NCF 0º had stronger anisotropic feature than the NCF ± 45º, it was stacked in the circumferential direction to further reinforce the mechanical properties in that direction. For the simulation, the mesh consisted of about 1.28 million tetrahedral elements and was built more finely in the complex region.

Table 1. Fiber volume fraction and permeability of the NCFs used in this study.

	NCF 0°	NCF ± 45°
Fiber volume fraction	0.416	0.425
K_{axial} ($\times 10^{-9}$ m^2)	2.149	3.573
$K_{trans.}$ ($\times 10^{-9}$ m^2)	1.221	
$K_{thick.}$ ($\times 10^{-12}$ m^2)	2.011	0.242

2.3. Materials and processing conditions

Epoxy resin (ρ = 1145 kg/m^3, μ = 0.5 Pa·s) was used as a liquid resin. The used carbon fiber (ρ = 1800 kg/m^3) was supplied by Toray® T700SC12K. The permeability tensor of each fabric was measured from our previous study as listed in Table 1.

The permeability and fiber volume fraction values were assigned to the elements. The distribution media was given a permeability of 10^{-7} in all the directions. To deal

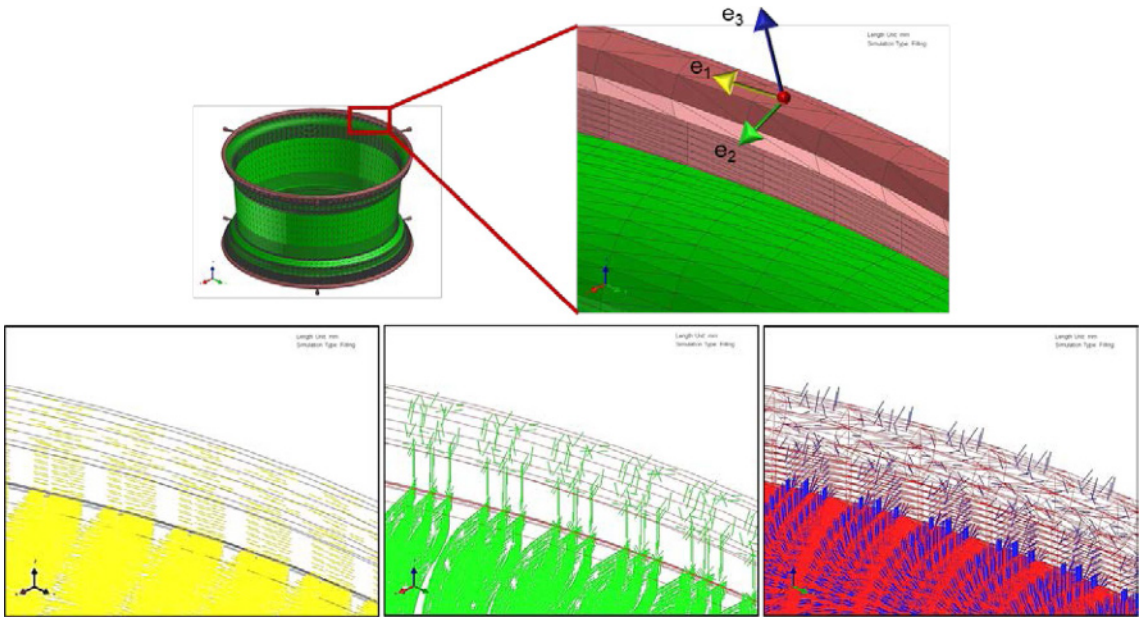

Fig. 4. (Color online) Local and global coordinates: e1, e2, and e3 indicate axial, transverse, and thickness directions in the local coordinate, respectively.

with the orientation of the fiber preform, the local coordinate systems were employed: Circumferential, axial, and radial axes (Fig. 4).

A constant inlet pressure of 2 bar was imposed. This value coincided with the experimental one. The inlet gates and outlet vents were marked by the navy and yellow arrows, respectively, as presented in Fig. 1a.

3. Results and Discussion

The numerical simulation was carried out to predict the resin flow behavior and the void content. Based on these results, the mold was designed, and the preforms were laminated. For the simulation, the following cases were considered:

Case 1: Narrow connection between the distribution medium and the thin preform.
Case 2: Wide connection between the distribution medium and the thin preform.
Case 3: Narrow connection between the distribution medium and the thick preform.
Case 4: Wide connection between the distribution medium and the thick preform.

The macro-void content is displayed in Fig. 5. Compared with Case 1, Case 2 showed the improved resin flow behavior such as the reduced filling time by means of widening the connection part. However, Case 3, which employed relatively thick preform and high content of NCF ± 45° with high permeability, showed the poor resin flow behavior such as the increased filling time. This indicates that the inlet geometry played a major role in determining the resin flow behavior in the filling stage. More detailed comparison was made between Case 1 and Case 4.

Figure 6 shows the flow front of resin at the given filling time for Case 1 and Case 4. The resin impregnated the distribution medium in several seconds and then flowed evenly along the z direction in both cases. The predicted total filling times were about 1091.1 s for Case 1 and 775.0 s for Case 4, respectively. Case 4 had a larger volume of the distribution medium than Case 1 because Case 1 employed the wide connection between the distribution medium and the preform. Therefore, Case 4 needed more time to fill the distribution medium at the beginning of filling stage than Case 1. However, the entire filling stage of Case 4 was facilitated more rapidly by the wide connection (Fig. 7).

Figure 8 shows the results of the macro-voids predicted numerically. Case 4 was found to have the significantly reduced void content compared to Case 1. As demon-

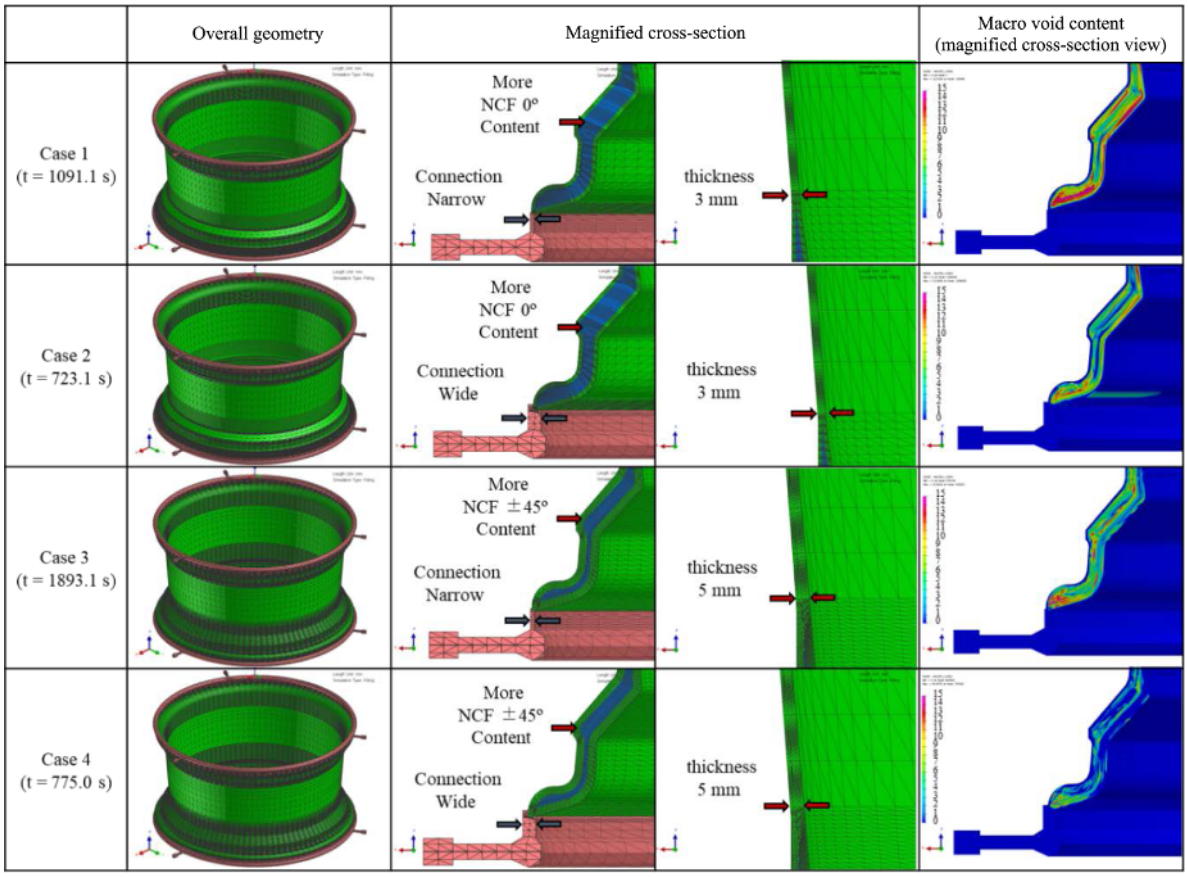

Fig. 5. (Color online) Geometry and macro-void content of the CFRP rims.

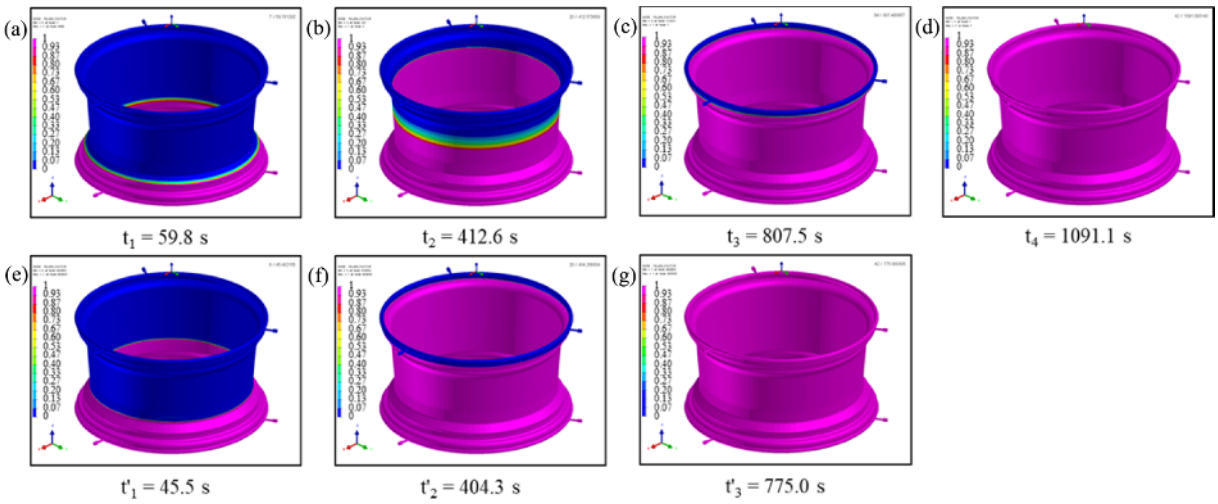

Fig. 6. (Color online) Numerical results of the flow front: (a) to (d) for Case 1 and (e) to (g) for Case 4.

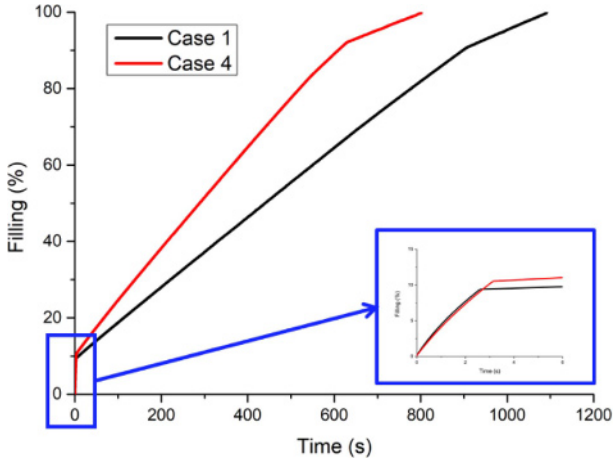

Fig. 7. (Color online) Filling percentage as a function of the time.

strated above, several differences between these two cases existed: The thickness of the connection part, the preform thickness, and the fabric layer structure. Hence, in order to minimize the void content not only the inlet geometry but also the fabric structure need to be controlled properly.

Based on the results of numerical simulation, the mold geometry and preform structure were upgraded. Considering Cases 1 and 4, two wheel rims were fabricated experimentally. Micro-CT measurement was carried out to observe the voids inside the manufactured products (Hwang *et al.*, 2015; Lee *et al.*, 2012). An X-ray Micro-CT system (Skyscan, 1172) was employed with 59 kV and 10 Mp X-ray source. The micro-CT system was used to perform 2D image analysis and realistic 3D visualization. As shown in Fig. 9, Case 4 had much lower void content than Case 1. Since one pixel size of the figure set as 11.55 μm, Fig. 9 shows all voids (including macro- and micro-voids) of a size larger than 11.55 μm. As it is difficult to distinguish macro-voids from micro-voids accurately, higher resolution was set and the micro-CT experiments were performed again. The shape of the fiber bundle can be confirmed, but the distinguishment between macro-

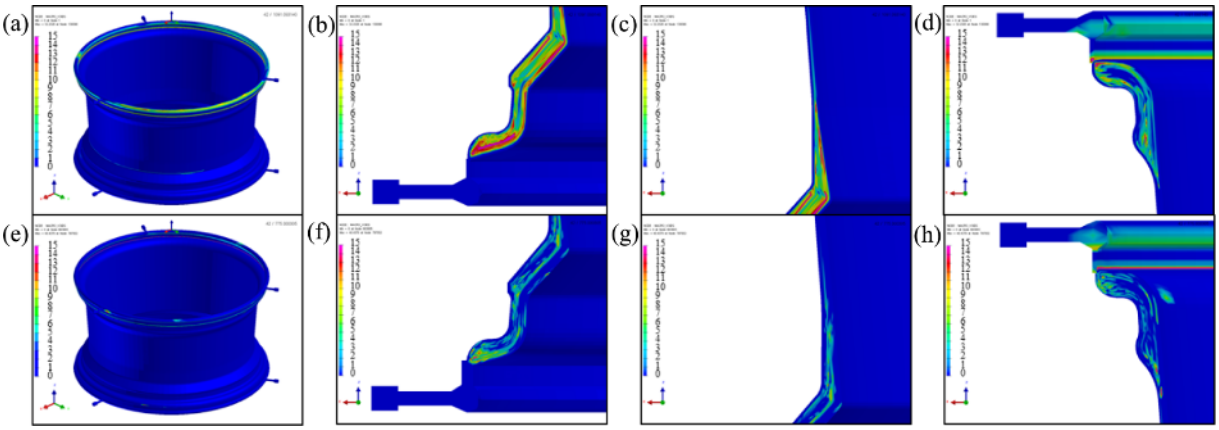

Fig. 8. (Color online) Overall and magnified cross-sectional views of the macro-void content calculated numerically: (a) to (d) for Case 1 and (e) to (h) for Case 4.

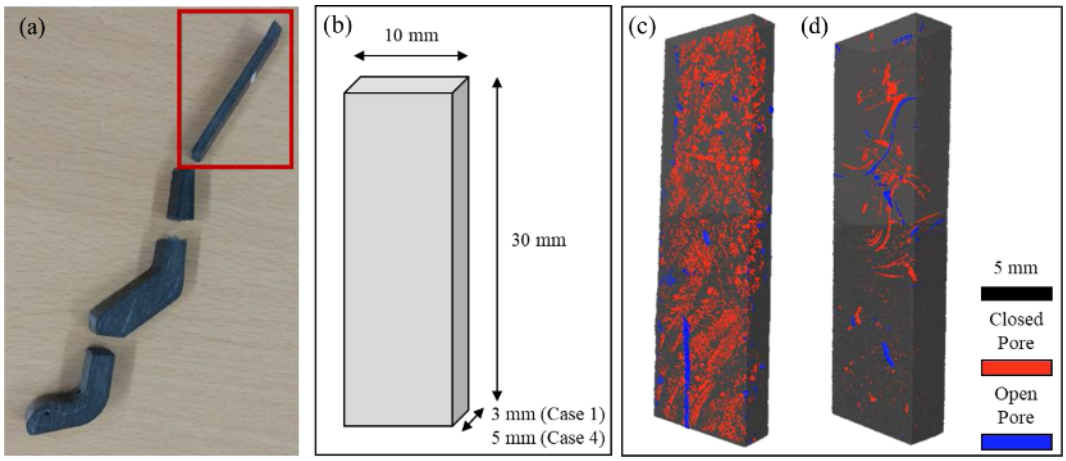

Fig. 9. (Color online) (a) Photograph of the sectioned parts from the produced wheel rim. (b) Dimensional details of the specimen for Micro-CT. Images of voids in the wheel rim: (c) for Case 1 and (d) for Case 4.

and micro-voids is still difficult at high resolution. Also, this study focused whether improvements have been made in several cases rather than distinguishing macro-voids from micro-voids. So, the experiments were conducted at normal resolution. The results indicate that numerical simulation is an efficient tool to optimize real manufacturing processes. In addition, the weight of the developed CFRP wheel is 10.5 kg, which is 25% lighter than conventional aluminum wheels with the same size. This suggests that CFRP composites are sufficiently applicable to the automotive wheels.

4. Conclusions

The 3D numerical analysis was performed to investigate the resin flow behavior during the RTM process. To improve the flow behavior and minimize the void formation, the mold geometry and the fabric structure were analyzed numerically. Based on the optimized numerical results, the automotive wheel rims were manufactured. The voids inside the manufactured CFRP wheels were measured by the micro-CT equipment. It was found that the numerical and experimental results were in good agreement with each other, and the numerical optimization led to significant improvement in the quality of the product.

Acknowledgements

This work was supported by GRRC program of Gyeonggi Province (GRRC Dankook2016–B03). In addition, this research was supported by Basic Science Research Program through the National Research Foundation of Korea (NRF) funded by the Ministry of Education (2018R1D1A1B07049173) and by the Korea government (MSIT) (No. NRF-2018R1A5A1024127). The authors are grateful for the supports.

References

Bruschke, M.V. and S.G. Advani, 1990, A finite element/control volume approach to mold filling in anisotropic porous media, *Polym. Compos.* **11**, 398-405.

Bruschke, M.V. and S.G. Advani, 1994, A numerical approach to model non-isothermal viscous flow through fibrous media with free surfaces, *Int. J. Numer. Methods Fluids* **19**, 575-603.

Chan, A.W. and S.T. Hwang, 1988, Mold-filling simulations for the injection molding of continuous fiber-reinforced polymer, *Polym. Eng. Sci.* **28**, 333-339.

Chan, A.W. and S.T. Hwang, 1991, Modeling of the impregnation process during resin transfer molding, *Polym. Eng. Sci.* **31**, 1149-1156.

Chan, A.W. and S.T. Hwang, 1992, Modeling nonisothermal impregnation of fibrous media with reactive polymer resin, *Polym. Eng. Sci.* **32**, 310-318.

Chen, J., Y.J. Dong, F.L. Jin, and S.J. Park, 2019, Flexural properties and electrical conductivity of epoxy resin/carbon fiber cloth/metallic powder composites, *Macromol. Res*. **27**, 10-13.

Coulter, J.P. and S.I. Guceri, 1988, Resin impregnation during the manufacturing of composite materials subject to prescribed injection rate, *J. Reinf. Plast. Compos.* **7**, 200-219.

García-Manrique, J.A., R. Hoto, L.I. Gascón, and J. Andrés, 2016, A numerical simulation of woven/anionic polyamide 6 composite part manufacturing using structural reactive injection moulding process, *J. Thermoplast. Compos. Mater.* **29**, 219-233.

Hattabi, M., J. Echaabi, and M.O. Bensalah, 2008, Numerical and experimental analysis of the resin transfer molding process, *Korea-Aust. Rheol. J.* **20**, 7-14.

Hwang, S.H., D.J. Lee, H.R. Youn, Y.S. Song, and J.R. Youn, 2015, Effects of fiber length distribution on flow property and internal microstructure of an injection molded part, *Macromol. Res.* **23**, 844-849.

Isoldi, L.A., C.P. Oliveira, L.A.O. Rocha, J.A. Souza, and S.C. Amico, 2012, Three-dimensional numerical modeling of RTM and LRTM processes, *J. Braz. Soc. Mech. Sci. Eng.* **34**, 105-

111.
Kim, B.Y., G.J. Nam, H.S. Ryu, and J.W. Lee, 2000, Optimization of filling process in RTM using genetic algorithm, *Korea-Aust. Rheol. J.* **12**, 83-92.
Laurenzi, S., A. Grilli, M. Pinna, F.D. Nicola, G. Cattaneo, and M. Marchetti, 2014, Process simulation for a large composite aeronautic beam by resin transfer molding, *Compos. Pt. B-Eng.* **57**, 47-55.
Lee, D.J., H. Oh, Y.S. Song, and J.R. Youn, 2012, Analysis of effective elastic modulus for multiphased hybrid composites, *Compos. Sci. Technol.* **72**, 278-283.
Lee, L.J., W.B. Young, and R.J. Lin, 1994, Mold filling and cure modeling of RTM and SRIM processes, *Compos. Struct.* **27**, 109-120.
Li, S. and R. Gauvin, 1991, Numerical analysis of the resin flow in resin transfer molding, *J. Reinf. Plast. Compos.* **10**, 314-327.
Lin, R.J., L.J. Lee, and M.J. Liou, 1993, Mold filling and curing analysis in liquid composite molding, *Polym. Compos.* **14**, 71-81.
Oliveira, I.R., S.C. Amico, J.A. Souza, and A.G.B. de Lima, 2015, Numerical analysis of the resin transfer molding process via PAM-RTM software, *Defect Diffus. Forum* **365**, 88-93.
Patel, N., V. Rohatgi, and L.J. Lee, 1995, Micro scale flow behavior and void formation mechanism during impregnation through a unidirectional stitched fiberglass mat, *Polym. Eng. Sci.* **35**, 837-851.
Poodts, E., G. Minak, L. Mazzocchetti, and L. Giorgini, 2014, Fabrication, process simulation and testing of a thick CFRP component using the RTM process, *Compos. Pt. B-Eng.* **56**, 673-680.
Ruiz, E., V. Achim, S. Soukane, F. Trochu, and J. Bréard, 2006, Optimization of injection flow rate to minimize micro/macro-voids formation in resin transfer molded composites, *Compos. Sci. Technol.* **66**, 475-486.
Shojaei, A., S.R. Ghaffarian, and S.M.H. Karimian, 2003, Modeling and simulation approaches in the resin transfer molding process: A review, *Polym. Compos.* **24**, 525-544.
Trochu, F., R. Gauvin, and D.M. Gao, 1993, Numerical analysis of the resin transfer molding process by the finite element method, *Adv. Polym. Technol.* **12**, 329-342.
Yim, Y.J., K.M. Bae, and S.J. Park, 2018, Influence of oxyfluorination on geometrical pull-out behavior of carbon-fiber-reinforced epoxy matrix composites, *Macromol. Res.* **26**, 794-799.
Yoo, Y.E. and W.I. Lee, 1996, Numerical simulation of the resin transfer mold filling process using the boundary element method, *Polym. Compos.* **17**, 368-374.
Young, W.B., 1994a, Gate location optimization in liquid composite molding using genetic algorithms, *J. Compos Mater.* **28**, 1098-1113.
Young, W.B., 1994b, Three-dimensional nonisothermal mold filling simulations in resin transfer molding, *Polym. Compos.* **15**, 118-127.
Young, W.B., K.H.L.H. Fong, and L.J. Lee, 1991a, Flow simulation in molds with preplaced fiber mats, *Polym. Compos.* **12**, 391-403.
Young, W.B., K. Rupel, K. Han, L.J. Lee, and M.J. Liou, 1991b, Analysis of resin injection molding in molds with preplaced fiber mats. II: Numerical simulation and experiments of mold filling, *Polym. Compos.* **12**, 30-38.